

Light-by-light scattering in ultraperipheral $PbPb$ collisions at the Large Hadron Collider

Mariola Kłusek-Gawenda,^{*} Piotr Lebiedowicz,[†] and Antoni Szczurek^{c§}

*Institute of Nuclear Physics, Polish Academy of Sciences,
Radzikowskiego 152, PL-31-342 Kraków, Poland*

(Dated: July 9, 2018)

Abstract

We calculate cross sections for diphoton production in (semi)exclusive $PbPb$ collisions, relevant for the LHC. The calculation is based on equivalent photon approximation in the impact parameter space. The cross sections for elementary $\gamma\gamma \rightarrow \gamma\gamma$ subprocess are calculated including two different mechanisms. We take into account box diagrams with leptons and quarks in the loops. In addition, we consider a vector-meson dominance (VDM-Regge) contribution with virtual intermediate hadronic (vector-like) excitations of the photons. We get much higher cross sections in $PbPb$ collisions than in earlier calculation from the literature. This opens a possibility to study the $\gamma\gamma \rightarrow \gamma\gamma$ (quasi)elastic scattering at the LHC. We present many interesting differential distributions which could be measured by the ALICE, CMS or ATLAS Collaborations at the LHC. We study whether a separation or identification of different components (boxes, VDM-Regge) is possible. We find that the cross section for elastic $\gamma\gamma$ scattering could be measured in the heavy-ion collisions for subprocess energies smaller than $W_{\gamma\gamma} \approx 15 - 20$ GeV.

PACS numbers: 25.75.Cj, 25.70.Bc, 34.50.-s

^c Also at University of Rzeszów, PL-35-959 Rzeszów, Poland.

^{*} Mariola.Klusek@ifj.edu.pl

[†] Piotr.Lebiedowicz@ifj.edu.pl

[§] Antoni.Szczurek@ifj.edu.pl

I. INTRODUCTION

In classical Maxwell theory photons/waves/wave packets do not interact. In contrast, in quantal theory they can interact via quantal fluctuations. So far only inelastic processes, i.e. production of hadrons or jets via photon-photon fusion could be measured e.g. in e^+e^- collisions [1–4]¹.

The light-by-light scattering to the leading and next-to-leading order was discussed earlier in the literature, see [5–7] also in the context of search for effects of new particles and interactions, e.g. see [8, 9]. The cross section for elastic $\gamma\gamma \rightarrow \gamma\gamma$ scattering is so small that till recently it was beyond the experimental reach. In e^+e^- collisions the energies and/or couplings of photons to electrons/positrons are rather small so that the corresponding $\gamma\gamma \rightarrow \gamma\gamma$ cross section is extremely small. A proposal to study helicity dependent $\gamma\gamma \rightarrow \gamma\gamma$ scattering in the region of MeV energies with the help of high power lasers was discussed recently e.g. in Ref. [10].

In proton-proton collisions the subprocess energies (diphoton invariant masses) can be larger and the underlying photon-photon scattering is possible in exclusive processes [11–13]. However, at low two-photon invariant masses there is a competitive diffractive QCD mechanism through the $gg \rightarrow \gamma\gamma$ subprocess with quark boxes [14–16] which gives much higher cross section than the photon-photon fusion [12]. The reader may find a detailed comparison of the two mechanisms in chapter 5 of [17]. The QCD mechanism provides an explanation of experimental cross sections measured by the CDF Collaboration [18, 19].

Ultrapерipheral collisions (UPC) of heavy-ions provide a nice possibility to study several two-photon induced processes such as: $\gamma\gamma \rightarrow l^+l^-$, $\gamma\gamma \rightarrow \pi^+\pi^-$, $\gamma\gamma \rightarrow$ dijets, etc. (see e.g. [20–22]). It was realized only recently that ultraperipheral heavy-ions collisions can be also a good place where photon-photon elastic scattering could be tested experimentally [11]. In Ref. [11] a first estimate of the corresponding cross section was presented.

In this paper we present a more detailed study with more realistic approach and show several differential distributions not discussed so far. We include also a new, higher order, mechanism not discussed so far in the literature.

II. $\gamma\gamma \rightarrow \gamma\gamma$ ELEMENTARY CROSS SECTION

Before presenting the nuclear cross sections let us concentrate first on elementary $\gamma\gamma \rightarrow \gamma\gamma$ scattering.

The lowest order QED mechanisms with elementary particles are shown in Fig. 1. The diagram in the left panel is for lepton and quark (elementary fermion) loops, while the diagram in the right panel is for W (spin-1) boson loops. The mechanism on the left hand side dominates at lower photon-photon energies while the mechanism on the right hand side becomes dominant at higher photon-photon energies (see e.g. [12, 23]). In numerical calculations here we include box diagrams with fermions only, which will be explained in the following.

The one-loop box diagrams were calculated by using the Mathematica package `FormCalc` [24] and the `LoopTools` library based on [25] to evaluate one-loop integrals. The com-

¹ Please note that here the incoming photons are virtual.

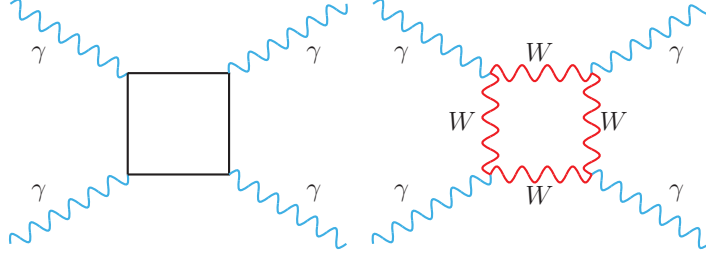


FIG. 1. Light-by-light scattering mechanisms with the lepton and quark loops (left panel) and as an example one topology of diagram for intermediate the W -boson loop (right panel).

plete matrix element was generated in terms of two-, three- and four-point coefficient functions [26], internally-defined photon polarisation vectors, and kinematic variables (four-momenta of incoming and outgoing photons). Our result was confronted with that in [6, 7, 23].

In principle, high-order contributions, not considered so far in the context of elastic scattering, are possible too. In Ref. [7] the authors considered both the QCD and QED corrections (two-loop Feynman diagrams) to the one-loop fermionic contributions in the ultrarelativistic limit ($\hat{s}, |\hat{t}|, |\hat{u}| \gg m_f^2$). The corrections are quite small numerically, showing that the leading order computations considered by us are satisfactory. In Fig. 2 (left panel) we show a process which is the same order in α_{em} but higher order in α_s . This mechanism is formally three-loop type and therefore difficult for calculation. We will not consider here the contribution of this three-loop mechanism. The exact three-loop calculation for this process is not yet available. Instead we shall consider “a similar” process shown in the right panel where both photons fluctuate into virtual vector mesons (three different light vector mesons are included). In this approach the interaction “between photons” happens when both photons are in their hadronic states.

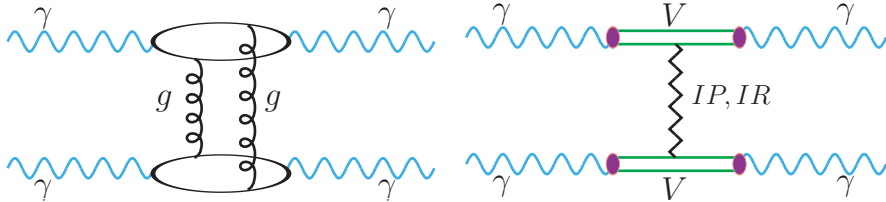


FIG. 2. Other elementary $\gamma\gamma \rightarrow \gamma\gamma$ processes. The left panel represents two-gluon exchange and the right panel is for VDM-Regge mechanism.

The differential cross section for the elementary $\gamma\gamma \rightarrow \gamma\gamma$ subprocess can be calculated as:

$$\frac{d\sigma_{\gamma\gamma \rightarrow \gamma\gamma}}{dt} = \frac{1}{16\pi s^2} \overline{|\mathcal{A}_{\gamma\gamma \rightarrow \gamma\gamma}|^2} \quad (2.1)$$

or

$$\frac{d\sigma_{\gamma\gamma \rightarrow \gamma\gamma}}{d\Omega} = \frac{1}{64\pi^2 s} \overline{|\mathcal{A}_{\gamma\gamma \rightarrow \gamma\gamma}|^2}. \quad (2.2)$$

In the most general case, including virtualities of initial photons, the amplitude can be written as: $\mathcal{A} = \mathcal{A}_{TT} + \mathcal{A}_{TL} + \mathcal{A}_{LT} + \mathcal{A}_{LL}$ where $\mathcal{A}_{TL} \propto \sqrt{Q_2^2}$, $\mathcal{A}_{LT} \propto \sqrt{Q_1^2}$, $\mathcal{A}_{LL} \propto$

$\sqrt{Q_1^2 Q_2^2}$. Since in UPC's $Q_1^2, Q_2^2 \approx 0$ (nuclear form factors kill large virtualities) the other terms can be safely neglected and $\mathcal{A} \approx \mathcal{A}_{TT}$.

The amplitude for the VDM-Regge contribution (see Fig. 2) can be written as²

$$\mathcal{A}_{\gamma\gamma \rightarrow \gamma\gamma}(s, t) \approx \left(\sum_{i=1}^3 C_{\gamma \rightarrow V_i}^2 \right) \mathcal{A}(s, t) \exp\left(\frac{B}{2}t\right) \left(\sum_{j=1}^3 C_{\gamma \rightarrow V_j}^2 \right), \quad (2.3)$$

where $i, j = \rho, \omega, \phi$. The $\gamma \rightarrow V$ transition constants are taken from [27] (see chapter 5, Eq. (1.11)). The amplitude for $V_i V_j \rightarrow V_i V_j$ elastic scattering is parametrized in the Regge approach similar as for $\gamma\gamma \rightarrow \rho^0 \rho^0$ in Ref. [28]

$$\mathcal{A}(s, t) \approx s \left((1+i) C_R \left(\frac{s}{s_0}\right)^{\alpha_R(t)-1} + i C_P \left(\frac{s}{s_0}\right)^{\alpha_P(t)-1} \right). \quad (2.4)$$

In all cases we assume the interaction parameters to be the same as for the $\pi^0 p$ interaction and obtained by the averaging:

$$\mathcal{A}_{\pi^0 p}(s, t) = \frac{1}{2} \left(\mathcal{A}_{\pi^+ p}(s, t) + \mathcal{A}_{\pi^- p}(s, t) \right). \quad (2.5)$$

Our amplitude here are normalized such that the optical theorem reads (for massless particles):

$$\sigma_{\pi p}^{tot}(s) = \frac{1}{s} \text{Im} \mathcal{A}_{\pi p}(s, t=0). \quad (2.6)$$

Some parameters ($C_{\gamma \rightarrow \rho^0}$, C_R , C_P) are also the same as for the VDM-Regge model for $\gamma\gamma \rightarrow \rho^0 \rho^0$ [28]. The parameters (C_R and C_P) are fixed assuming Regge factorization and the Donnachie-Landshoff parametrizations [29] of the NN and πN total cross sections (see e.g. [30, 31]). The slope parameter (see Eq. (2.3)), in general a free parameter, should be similar as for the pion-pion (dipole-dipole) scattering. For a simple estimate here we take $B = 4 \text{ GeV}^{-2}$ as in our previous paper on double ρ^0 production [28].

The elementary angle-integrated cross section for the box and VDM-Regge contributions is shown in Fig. 3 as a function of the photon-photon subsystem energy. Lepton and quark amplitudes interfere in cross section for the box contribution. For instance in the $4 < W < 50 \text{ GeV}$ region, neglecting interference effects, the lepton contribution to the box cross section is by a factor 5 bigger than the quark contribution. Interference effects are, however, large and cannot be neglected. At energies $W > 30 \text{ GeV}$ the VDM-Regge cross section becomes larger than that for the box diagrams. Can this be seen/identified in heavy ion lead-lead collisions at the LHC including experimental cuts? We will try to answer this question in this paper.

For completeness in Fig. 4 we show also differential cross section for the box (left panel) and the VDM-Regge (right panel) components as a function of subsystem energy and photon transverse momentum. The distribution for the box mechanism (left panel) has a characteristic enhancement for $p_{t,\gamma} \approx W/2$ which is due to jacobian of variables transformation from finite $d\sigma/dz$ distribution at $z = 0$. One can observe a fast fall-off

² In fact the helicity amplitude can be written as $A_{\lambda_1 \lambda_2 \rightarrow \lambda_3 \lambda_4} = \delta_{\lambda_1 \lambda_3} \delta_{\lambda_2 \lambda_4} \cdot A$

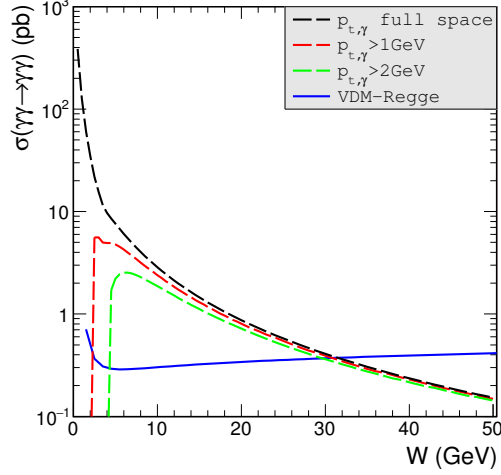


FIG. 3. Integrated $\gamma\gamma \rightarrow \gamma\gamma$ cross section as a function of the subsystem energy. The dashed lines show contribution of boxes and the solid line represents result of the VDM-Regge mechanism.

of the differential cross section with photon transverse momenta for the VDM-Regge mechanism (right panel). Imposing lower $p_{t,\gamma}$ cuts in experiments would therefore almost completely kill the VDM-Regge contribution. We expect that compared to our soft VDM-Regge component the two-gluon exchange component (see the left panel of Fig. 2) should have larger wings/tails at larger transverse momenta. This may be a bit academic problem but may be interesting by itself.

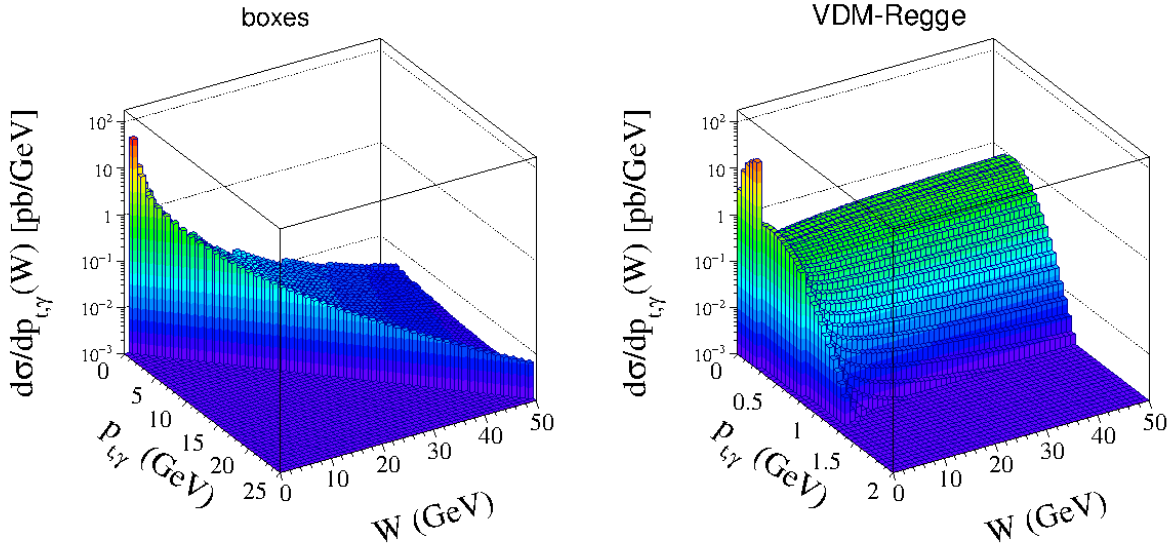


FIG. 4. Elementary cross section $d\sigma/dp_{t,\gamma}$ as a function of the subprocess energy W ($\gamma\gamma$ invariant mass in the nuclear process) and transverse momentum of one of the outgoing photons for the box (left panel) and VDM-Regge (right panel) mechanisms.

Fig. 5 presents two-dimensional distribution of the elementary $\gamma\gamma \rightarrow \gamma\gamma$ cross section as a function of cosine of the angle between outgoing photons $z = \cos\theta$ and energy.

The left panel shows distribution for the box mechanism and the right panel is for the VDM-Regge mechanism. For both cases, the largest cross section occurs at $z \approx \pm 1$.

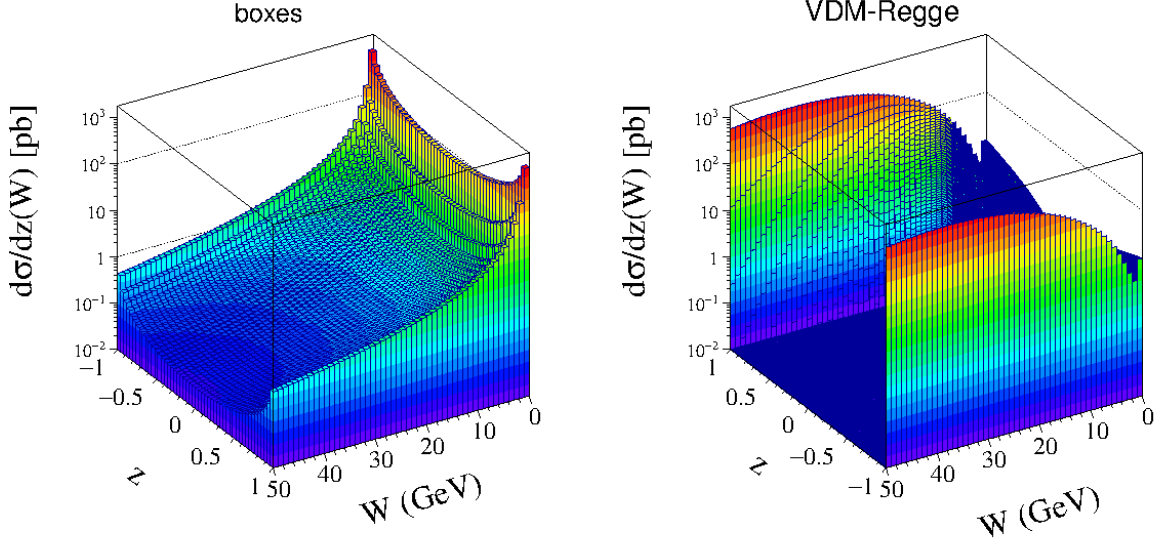


FIG. 5. Elementary cross section $d\sigma/dz$ as a function of the subprocess energy W ($\gamma\gamma$ invariant mass in the nuclear process) and $z = \cos \theta$ for the box (left panel) and VDM-Regge (right panel) mechanisms.

Now we shall proceed to nuclear calculations where the elementary cross sections discussed above are main ingredients of the approach.

III. DIPHOTON PRODUCTION IN UPC OF HEAVY IONS

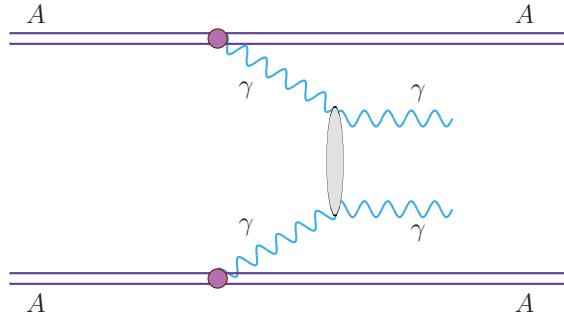


FIG. 6. $AA \rightarrow AA\gamma\gamma$ in ultrarelativistic UPC of heavy ions.

The general situation for $AA \rightarrow AA\gamma\gamma$ is sketched in Fig. 6. Here we follow our earlier approach applied already to different reactions [28, 32–37]. In our equivalent photon approximation in the impact parameter space, the total (phase space integrated) cross

section is expressed through the five-fold integral (for more details see e.g. [32])

$$\begin{aligned} \sigma_{A_1 A_2 \rightarrow A_1 A_2 X}(\sqrt{s_{A_1 A_2}}) &= \int \sigma_{\gamma\gamma \rightarrow \gamma\gamma}(\sqrt{s_{A_1 A_2}}) N(\omega_1, \mathbf{b}_1) N(\omega_2, \mathbf{b}_2) S_{abs}^2(\mathbf{b}) \\ &\times 2\pi b db d\bar{b}_x d\bar{b}_y \frac{W_{\gamma\gamma}}{2} dY_{\gamma\gamma}, \end{aligned} \quad (3.1)$$

where $N(\omega_i, \mathbf{b}_i)$ are photon fluxes³ and

$$Y_{\gamma\gamma} = \frac{1}{2} (y_{\gamma_1} + y_{\gamma_2}) \quad (3.2)$$

is a rapidity of the outgoing $\gamma\gamma$ system. The invariant mass of the $\gamma\gamma$ system is defined as

$$W_{\gamma\gamma} = \sqrt{4\omega_1\omega_2}, \quad (3.3)$$

where $\omega_{1/2} = W_{\gamma\gamma}/2 \exp(\pm Y_{\gamma\gamma})$. The quantities \bar{b}_x, \bar{b}_y are the components of the \mathbf{b}_1 and \mathbf{b}_2 vectors:

$$\mathbf{b}_1 = \left[\bar{b}_x + \frac{b}{2}, \bar{b}_y \right], \quad \mathbf{b}_2 = \left[\bar{b}_x - \frac{b}{2}, \bar{b}_y \right]. \quad (3.4)$$

Eq. (3.1) allows to calculate total cross section, distributions in the impact parameter ($b = b_m$), invariant mass of the diphoton system ($W_{\gamma\gamma} = M_{\gamma\gamma}$) or rapidity of the pair ($Y_{\gamma\gamma}$) of these particles. $S_{abs}^2(b)$ is a geometrical factor which takes into account survival probability of nuclei as a function of impact parameter. To a reasonable approximation it can be approximated as

$$S_{abs}^2(b) = \theta(b - (R_A + R_B)). \quad (3.5)$$

If one wishes to impose some cuts on produced particles (photons) which come from experimental requirements or to have distribution in some helpful and interesting kinematical variables of individual particles (here photons), a more complicated calculations are required. Then we have to introduce into the integration an additional dimension related to angular distribution for the subprocess (e.g. $z = \cos \theta$ or $p_{t,\gamma}$). Then we define kinematical variables of photons in the $\gamma\gamma$ center-of-mass system (denoted here by *):

$$E_{\gamma_i}^* = p_{\gamma_i}^* = \frac{W_{\gamma\gamma}}{2}, \quad (3.6)$$

$$z = \cos \theta^* = \sqrt{1 - \left(\frac{p_{t,\gamma}}{p_{\gamma_i}^*} \right)^2}, \quad (3.7)$$

$$p_{z,\gamma_i}^* = \pm z p_{\gamma_i}^*, \quad (3.8)$$

$$y_{\gamma_i}^* = \frac{1}{2} \ln \frac{E_{\gamma_i}^* + p_{z,\gamma_i}^*}{E_{\gamma_i}^* - p_{z,\gamma_i}^*} \quad (3.9)$$

and in overall AA center of mass system:

$$y_{\gamma_i} = Y_{\gamma\gamma} + y_{\gamma_i}^*, \quad (3.10)$$

$$p_{z,\gamma_i} = p_{t,\gamma} \sinh(y_{\gamma_i}), \quad (3.11)$$

$$E_{\gamma_i} = \sqrt{p_{z,\gamma_i}^2 + p_{t,\gamma}^2}, \quad (3.12)$$

where $i = 1, 2$ means first or second outgoing photon, respectively.

³ Nuclear charge form factors are main ingredients of the photon flux[32].

IV. FIRST RESULTS

cuts	boxes		VDM-Regge	
	$F_{realistic}$	$F_{monopole}$	$F_{realistic}$	$F_{monopole}$
$W_{\gamma\gamma} > 5 \text{ GeV}$	306	349	19	22
$W_{\gamma\gamma} > 5 \text{ GeV}, p_{t,\gamma} > 2 \text{ GeV}$	159	182	7E-9	8E-9
$E_{\gamma} > 3 \text{ GeV}$	16 692	18 400	13	14
$E_{\gamma} > 5 \text{ GeV}$	4 800	5 450	4	6
$E_{\gamma} > 3 \text{ GeV}, y_{\gamma_i} < 2.5$	183	210	7E-2	8E-2
$E_{\gamma} > 5 \text{ GeV}, y_{\gamma_i} < 2.5$	54	61	3E-4	6E-4
$p_{t,\gamma} > 0.9 \text{ GeV}, y_{\gamma_i} < 0.7 \text{ (ALICE cuts)}$	107			
$p_{t,\gamma} > 5.5 \text{ GeV}, y_{\gamma_i} < 2.5 \text{ (CMS cuts)}$	10			

TABLE I. Integrated cross sections in nb for exclusive diphoton production processes with both photons measured for $\sqrt{s_{NN}} = 5.5 \text{ TeV}$ (LHC). The calculations was performed within impact-parameter EPA. The values of the total cross sections are shown for different cuts on kinematic variables.

To illustrate the general situation in Table I we have collected integrated cross sections corresponding to different kinematical cuts. Here we show results for the two (boxes, VDM-Regge) mechanisms separately⁴ for very different kinematical situation. In all cases considered the cross section obtained with the monopole form factor is by more than 10% bigger than that obtained with the realistic form factor (Fourier transform of nucleus charge distribution). In the first row we show results for cuts from Ref. [11]. We get much larger cross section than that found in [11] ($\sigma = 35 \pm 7 \text{ nb}$). In this case the VDM-Regge contribution not considered in earlier calculations constitutes about 7% of the dominant box contribution. Already the cut on transverse momentum of photons as large as $p_{t,\gamma} > 2 \text{ GeV}$ completely kills the VDM-Regge contribution which is very forward/backward peaked. For the box contribution the effect is much smaller. The cut on photon-photon energies is not necessary. If we impose only cuts on energy of photons in the overall (nucleus-nucleus) center-of-mass system (laboratory frame) the box-contribution is much larger, of the order of microbarns. However, restricting to the rapidity coverage of the main detector diminishes the cross sections considerably, especially for the VDM-Regge contribution. The explanation will become clear when discussing differential distributions below.

In Fig. 7 we show results which can be obtained by calculating five-fold integral (see Eq.(3.1)). In this calculation we have imposed only a lower cut (5.5 GeV) on photon-photon energy (or diphoton invariant mass) to get rid of the resonance region which may be more complicated. Each of distributions (in b_m , $M_{\gamma\gamma}$, $Y_{\gamma\gamma}$ for boxes and VDM-Regge) is shown for the case of realistic charge density and monopole form factor in nuclear calculations. The difference between the results becomes larger with larger values of the kinematical variables. The cross section obtained with the monopole form factor is larger for each case. The distribution in impact parameter, purely theoretical (cannot be checked experimentally), quickly drops with growing impact parameter. The distribution in invariant mass seems rather interesting. While at low invariant masses the box

⁴ By doing so we neglect possible interference effects between the two mechanisms.

contribution wins, at invariant masses $M_{\gamma\gamma} > 30$ GeV the VDM-Regge contribution is bigger. Can we thus observe experimentally the VDM-Regge contribution? The matter is a bit more complicated as will be explained below. The distribution in diphoton rapidity is a bit academic and in fact confusing for the VDM-Regge contribution and may wrongly suggest that all photons are produced at midrapidities. We shall discuss this in detail in the following.

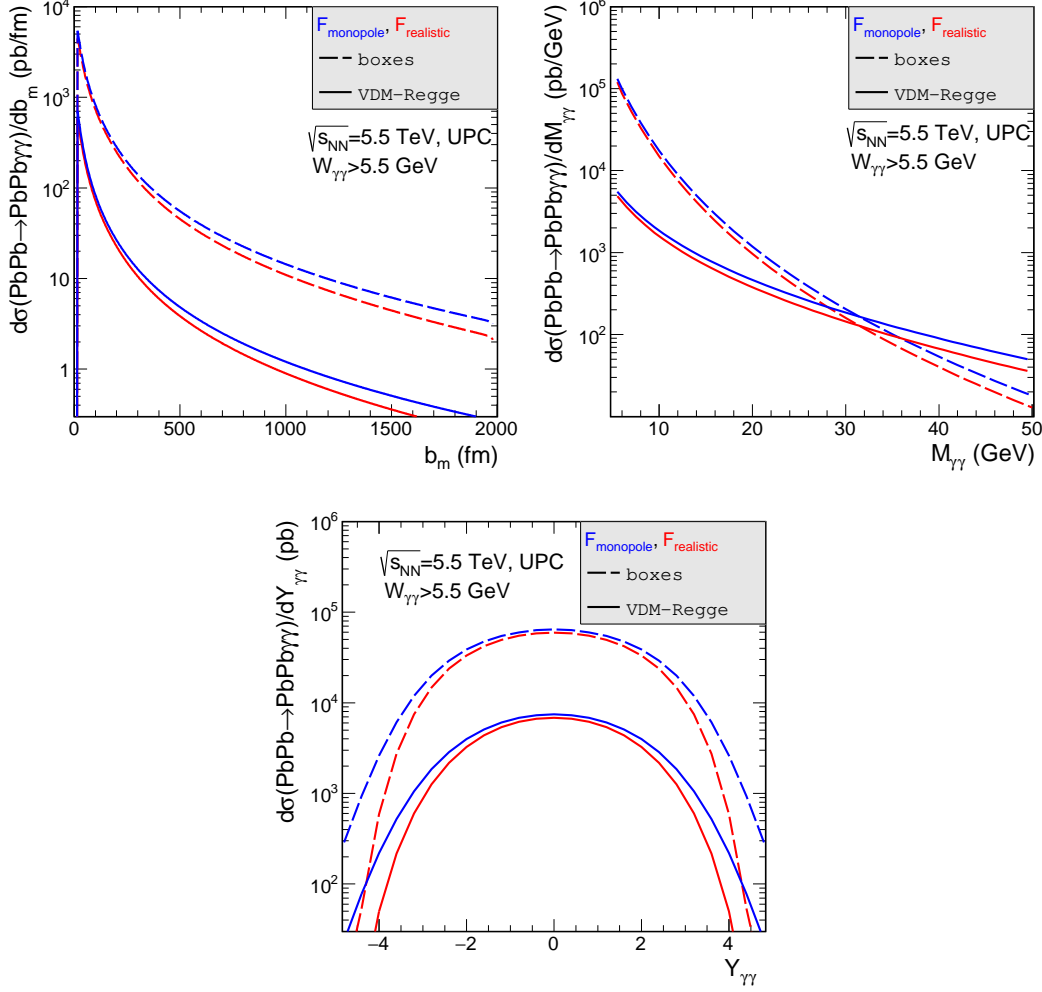


FIG. 7. Predictions for the $\text{PbPb} \rightarrow \text{PbPb}\gamma\gamma$ reaction in UPC of heavy ions. Differential nuclear cross section as a function of impact parameter, $\gamma\gamma$ invariant mass and rapidity of photon pairs at $\sqrt{s_{NN}} = 5.5$ TeV and with extra cut on $W_{\gamma\gamma} > 5.5$ GeV. The distributions with realistic charge density are depicted by the red (lower) lines and the distributions which are calculated using monopole form factor are shown by the blue (upper) lines. The dashed lines show the results for the case when only box contributions (fermion loops) are included. The solid lines show the results for the VDM-Regge mechanism.

Can something be measured with the help of LHC detectors? In Fig. 8 we show numbers of counts in the 1 GeV intervals expected for assumed integrated luminosity of 1 nb^{-1} , where in addition to the lower cut on photon-photon energy we have imposed cuts on (pseudo)rapidities of both photons. It looks that one can get (measure) invariant

mass distribution up to $M_{\gamma\gamma} \approx 15$ GeV. This is much more than predicted previously in Ref. [11]. We do not have clear explanation of the difference.

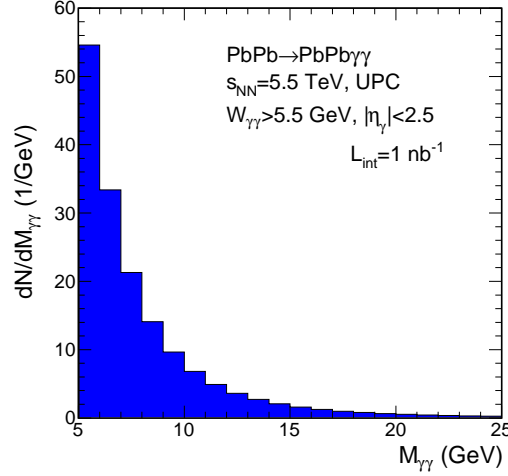


FIG. 8. Distribution of expected number of counts in 1 GeV bins for cuts specified in the figure legend. This figure should be compared with a similar figure in [11].

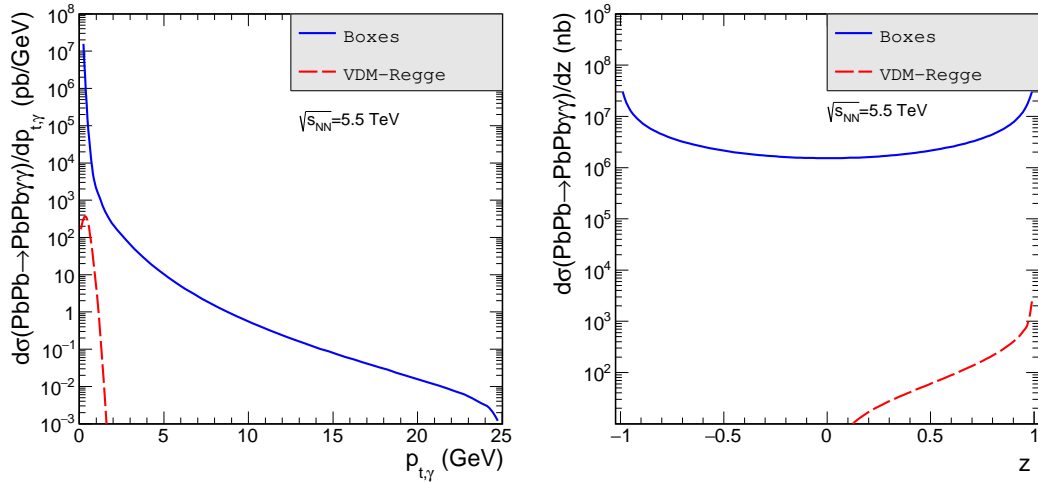


FIG. 9. Results for the $\text{PbPb} \rightarrow \text{PbPb} \gamma \gamma$ reaction in UPC of heavy ions. Differential nuclear cross section as a function of photon transverse momentum $p_{t,\gamma}$ and cosine of the angle between outgoing photons $z = \cos \theta^*$ at $\sqrt{s_{NN}} = 5.5$ TeV with minimal cut on $M_{\gamma\gamma} > 1$ GeV for the VDM-Regge mechanism only. The solid lines show the results for the case when only box contributions (fermionic loops) are included. The dashed lines show the results for the VDM-Regge approach only.

Now we wish to show some selected results with essentially no cuts except of a minimal cut to assure that the VDM-Regge model applies. Fig. 9 shows differential cross section as a function of photon transverse momentum $p_{t,\gamma}$ (left panel) and cosine of the angle between outgoing photons $z = \cos \theta^*$ (right panel). The calculations are done at the

LHC energy $\sqrt{s_{NN}} = 5.5$ TeV. Here we impose no cuts on kinematical variables for box contribution and VDM-Regge mechanism except $M_{\gamma\gamma} > 1$ GeV condition. We know that the VDM-Regge mechanism does not apply below this value. One can observe that the nuclear $d\sigma/dp_{t,\gamma}$ distribution falls very quickly for both mechanisms and is very narrow for the VDM-Regge contribution. The distribution in z (right panel) shows that without cuts on kinematical variables the maximal cross section occurs at $z \approx \pm 1$. We show only one half of the z distribution for the VDM-Regge approach, because we include only contribution from the t channel in our calculation. Contribution from the u channel should have similar shape of distribution but for the second half of the z distribution and would be symmetric to the t -channel contribution around the $z = 0$. We see that already for $W_{\gamma\gamma} = M_{\gamma\gamma} > 1$ GeV it is not necessary to symmetrize the t and u diagrams.

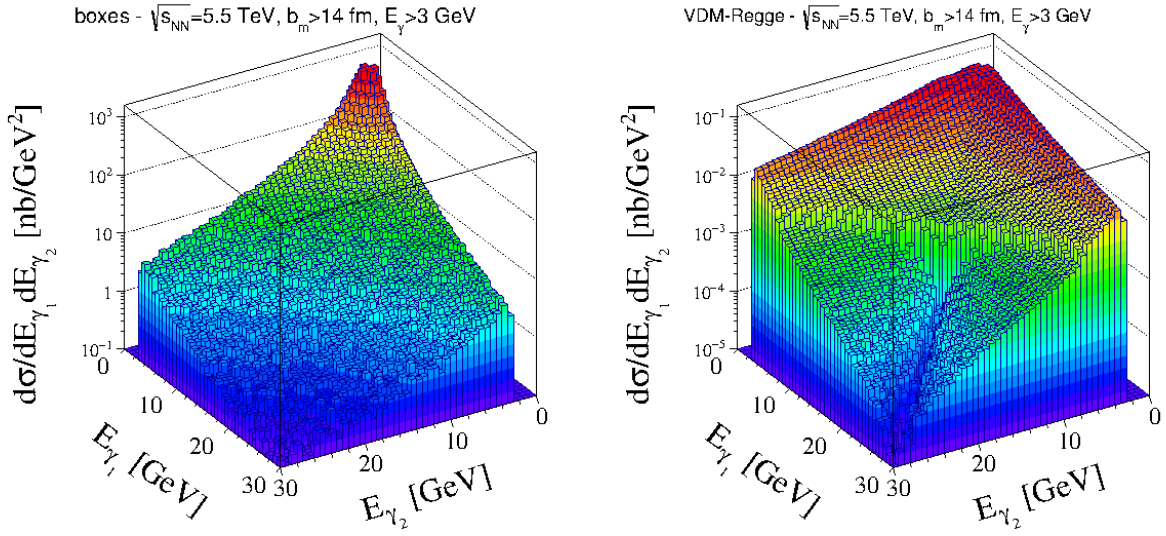


FIG. 10. Two-dimensional distribution in energies of the two photons in the laboratory frame for box (left panel) and VDM-Regge (right panel) contributions.

The cuts on photon-photon energies are in principle not necessary. What are in fact energies of photons in the laboratory frame of reference? In Fig. 10 we show distribution of energies of both photons, separately for the two mechanisms: boxes (left panel) and VDM-Regge (right panel). In this calculations we do not impose cuts on $W_{\gamma\gamma}$ but only minimal cuts on energies of individual photons ($E_\gamma > 3$ GeV) in the laboratory frame. Slightly different distributions are obtained for boxes and VDM-Regge mechanisms. For the box mechanism we can observe a pronounced maximum when both energies are small. For both mechanisms the maximum of the cross section occurs for rather asymmetric configurations: $E_1 \gg E_2$ or $E_1 \ll E_2$.

Two-dimensional distributions in photon rapidities are very different for the box and VDM-Regge contributions (Fig. 11). In the case of the VDM-Regge contribution we observe as if non continuous behaviour (dip in the cross section, better visible in Fig. 12 where we show projections on both axes) which is caused by the strong transverse momentum dependence of the elementary cross section (see Fig. 4) which causes that some regions in the two-dimensional space are almost not populated.

In Fig. 13 we show the same distributions in the contour representation with the ex-

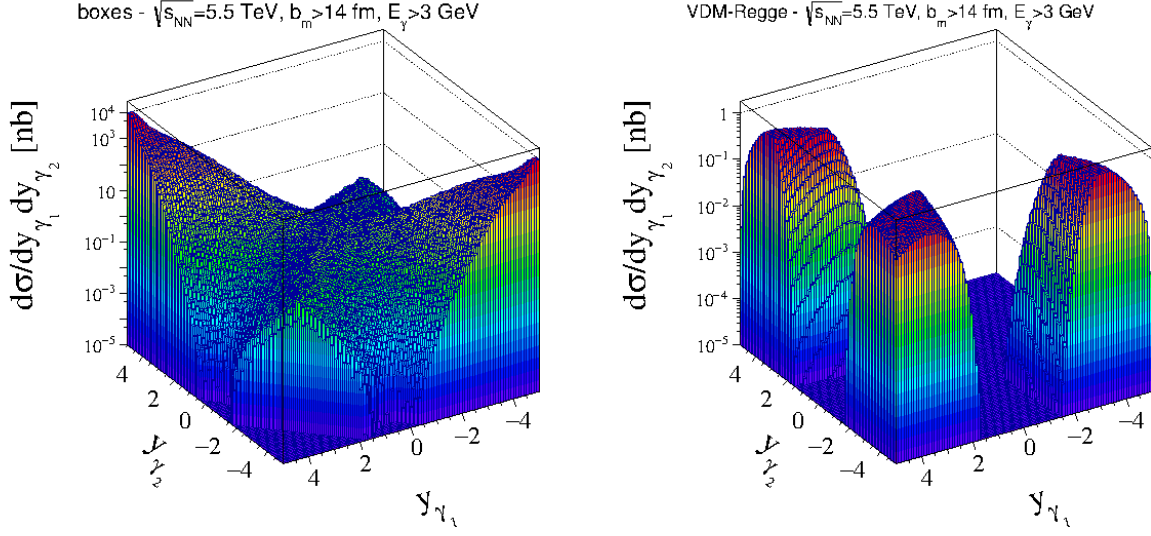


FIG. 11. Two-dimensional distribution in rapidities of the two photons in the laboratory frame for box (left panel) and VDM-Regge (right panel) contributions.

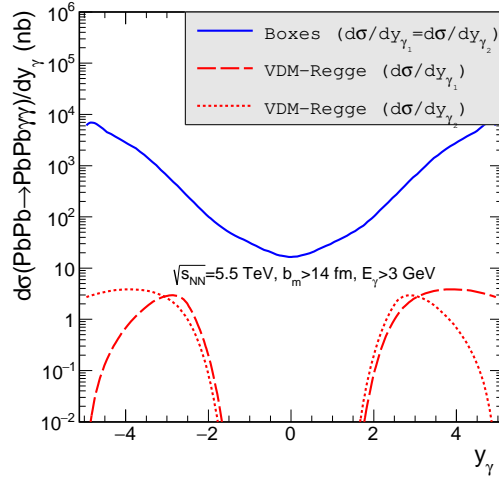


FIG. 12. Projection on rapidity of one of the photons. The cuts here are the same as in Fig. 11. For the VDM contribution, the dashed and dotted lines are projections on the y_{γ_1} and y_{γ_2} axes, respectively.

perimental limitations ($y_{\gamma_1}, y_{\gamma_2} \in (-2.5, 2.5)$) of the main detectors. For the case of the VDM-Regge contribution we show distribution for only one half of the $(y_{\gamma_1}, y_{\gamma_2})$ space. Clearly the VDM-Regge contribution does not fit to the main detector and extends towards large rapidities. Could photons originating from this mechanism be measured with the help of so-called zero-degree calorimeters (ZDCs) associated with the ATLAS or CMS main detectors?

In Fig. 14 we show the VDM-Regge contribution in much broader range of rapidity. Now we discover that maxima of the cross section associated with this mechanism are

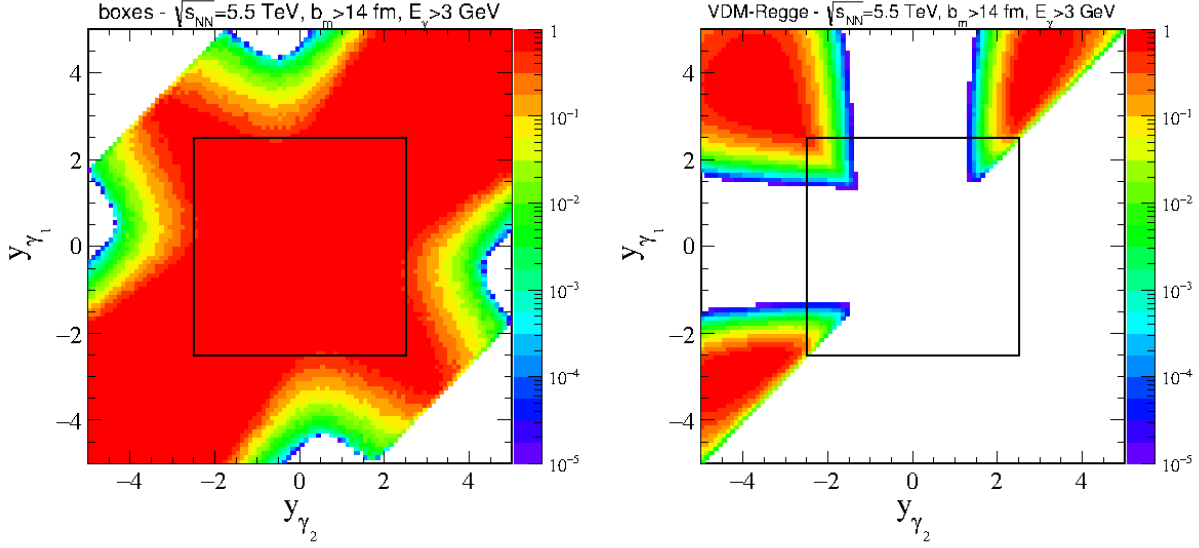


FIG. 13. Contour representation of two-dimensional distribution in rapidities of the two photons in the laboratory frame for box (left panel) and VDM-Regge (right panel) contributions with shown experimental rapidity coverage of the main the ATLAS or CMS detectors. Only one half of the $(y_{\gamma_1}, y_{\gamma_2})$ space is shown for the VDM-Regge contribution. The second half can be obtained from the symmetry around the $y_{\gamma_1} = y_{\gamma_2}$ line.

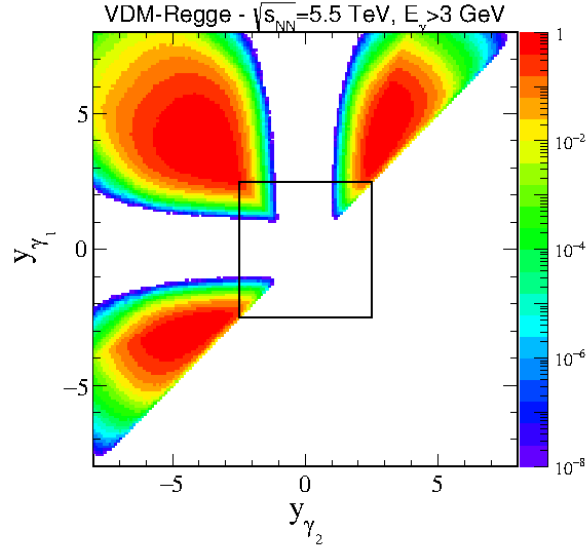


FIG. 14. Contour representation of two-dimensional distribution in rapidities of the two photons in the laboratory frame for the VDM-Regge contribution in the extended range of rapidities. Only one half of the $(y_{\gamma_1}, y_{\gamma_2})$ space is shown explicitly. The second half can be obtained from the symmetry around the $y_{\gamma_1} = y_{\gamma_2}$ line.

at $|y_{\gamma_1}|, |y_{\gamma_2}| \approx 5$. Unfortunately this is below the limitations of the ZDCs $|\eta| > 8.3$ for ATLAS ([38]) or 8.5 for CMS ([39]).

V. CONCLUSIONS

We have performed detailed feasibility studies of elastic photon-photon scattering in ultraperipheral heavy ion collisions at the LHC. The calculation was performed in equivalent photon approximation in the impact parameter space. This method allows to remove those cases when nuclei collide and therefore break apart. Such cases are difficult in interpretation and were omitted here.

The cross section for elementary photon-photon scattering has been calculated including box diagrams with elementary Standard Model particles as well as a new component called here "VDM-Regge" for brevity. This soft component is based on the idea of hadronic fluctuation of the photon(s). The photons interact when they are in their hadronic (virtual vector meson) states. The standard soft Regge phenomenological type of interaction is used for the hadron-hadron interaction. The VDM-Regge mechanism gives in general much smaller cross section but for $W_{\gamma\gamma} > 30$ GeV starts to dominate over the box contributions, at least in the full phase space.

Several distributions in the "standard" EPA were calculated. The results were compared to results of earlier calculation in the literature. We have found cross sections by a factor of about 8 bigger than previously published in the literature. We have made an estimate of the counting rate with expected integrated luminosity. We expect some counts ($N > 1$) for $W_{\gamma\gamma} = M_{\gamma\gamma} < 15\text{-}20$ GeV.

We have performed a detailed calculation including also distributions of individual outgoing photons by extending the standard EPA. We have made estimation of the integrated cross section for different experimental situations relevant for the ALICE or CMS experiments as well as shown several differential distributions. We have studied whether the VDM-Regge component, not discussed so far, could be identified experimentally and have shown that it will be probably very difficult.

We have found that, very different than for the box contribution, the VDM-Regge contribution reaches a maximum of the cross section when $(y_{\gamma_1} \approx 5, y_{\gamma_2} \approx -5)$ or $(y_{\gamma_1} \approx -5, y_{\gamma_2} \approx 5)$. This is a rather difficult region which cannot be studied e.g. with ZDC's installed at the LHC.

So far we have studied only diphoton continuum. The resonance mechanism could be also included in the future. In the present studies we have concentrated on the signal. Future studies should include also estimation of the background. The dominant background may be expected from the $AA \rightarrow AAe^+e^-$ when both electrons are misidentified as photons.

Acknowledgments

This work was partially supported by the Polish grant No. DEC-2014/15/B/ST2/02528 (OPUS) as well as by the Centre for Innovation and Transfer of Natural Sciences and Engineering Knowledge in Rzeszów. A part of the calculations within this analysis was carried out with the help of the cloud computer system (Cracow Cloud One⁵) of the Institute of Nuclear Physics PAN.

⁵ cc1.ifj.edu.pl

-
- [1] D. Buskulic *et al.*, (ALEPH Collaboration), *An Experimental study of $\gamma\gamma \rightarrow \text{hadrons}$ at LEP*, Phys. Lett. **B313** (1993) 509–519.
 - [2] K. Muramatsu *et al.*, (TOPAZ Collaboration), *Measurement of the photon structure function $F_2(\gamma)$ and jet production at TRISTAN*, Phys. Lett. **B332** (1994) 477–487.
 - [3] K. Ackerstaff *et al.*, (OPAL Collaboration), *Inclusive jet production in photon-photon collisions at $\sqrt{s} = 130\text{-GeV}$ and 136-GeV* , Z. Phys. **C73** (1997) 433–442.
 - [4] R. Barate *et al.*, (ALEPH Collaboration), *Study of fermion pair production in e^+e^- collisions at 130-GeV to 183-GeV* , Eur. Phys. J. **C12** (2000) 183–207, arXiv:hep-ex/9904011 [hep-ex].
 - [5] M. Bohm and R. Schuster, *Scattering of light by light in the electroweak standard model*, Z. Phys. **C63** (1994) 219–225.
 - [6] G. Jikia and A. Tkabladze, *Photon-photon scattering at the photon linear collider*, Phys. Lett. **B323** (1994) 453–458, arXiv:hep-ph/9312228 [hep-ph].
 - [7] Z. Bern, A. De Freitas, L. J. Dixon, A. Ghinculov, and H. L. Wong, *QCD and QED corrections to light by light scattering*, JHEP **11** (2001) 031, arXiv:hep-ph/0109079 [hep-ph].
 - [8] G. J. Gounaris, P. I. Porfyriadis, and F. M. Renard, *Light by light scattering at high-energy: A Tool to reveal new particles*, Phys. Lett. **B452** (1999) 76–82, arXiv:hep-ph/9812378 [hep-ph].
 - [9] G. J. Gounaris, P. I. Porfyriadis, and F. M. Renard, *The $\gamma\gamma \rightarrow \gamma\gamma$ process in the standard and SUSY models at high-energies*, Eur. Phys. J. **C9** (1999) 673–686, arXiv:hep-ph/9902230 [hep-ph].
 - [10] K. Homma, K. Matsuura, and K. Nakajima, *Testing helicity dependent $\gamma\gamma \rightarrow \gamma\gamma$ scattering in the region of MeV*, arXiv:1505.03630 [hep-ex].
 - [11] D. d’Enterria and G. G. da Silveira, *Observing light-by-light scattering at the Large Hadron Collider*, Phys. Rev. Lett. **111** (2013) 080405, arXiv:1305.7142 [hep-ph].
 - [12] P. Lebiedowicz, R. Pasechnik, and A. Szczurek, *Search for technipions in exclusive production of diphotons with large invariant masses at the LHC*, Nucl. Phys. **B881** (2014) 288–308, arXiv:1309.7300 [hep-ph].
 - [13] S. Fichtel, G. von Gersdorff, O. Kepka, B. Lenzi, C. Royon, and M. Saimpert, *Probing new physics in diphoton production with proton tagging at the Large Hadron Collider*, Phys. Rev. **D89** (2014) 114004, arXiv:1312.5153 [hep-ph].
 - [14] V. A. Khoze, A. D. Martin, M. G. Ryskin, and W. J. Stirling, *Diffractional gamma-gamma production at hadron colliders*, Eur. Phys. J. **C38** (2005) 475–482, arXiv:hep-ph/0409037 [hep-ph].
 - [15] P. Lebiedowicz, R. Pasechnik, and A. Szczurek, *QCD diffractional mechanism of exclusive W^+W^- pair production at high energies*, Nucl. Phys. **B867** (2013) 61–81, arXiv:1203.1832 [hep-ph].
 - [16] L. A. Harland-Lang, V. A. Khoze, M. G. Ryskin, and W. J. Stirling, *Central exclusive production within the Durham model: a review*, Int. J. Mod. Phys. **A29** (2014) 1430031, arXiv:1405.0018 [hep-ph].
 - [17] P. Lebiedowicz, *Exclusive reactions with light mesons: From low to high energies*. http://www.ifj.edu.pl/msd/rozprawy_dr/rozpr_Lebiedowicz.pdf, 2014.
 - [18] T. Aaltonen *et al.*, (CDF Collaboration), *Search for exclusive $\gamma\gamma$ production in hadron-hadron collisions*, Phys. Rev. Lett. **99** (2007) 242002, arXiv:0707.2374 [hep-ex].
 - [19] T. Aaltonen *et al.*, (CDF Collaboration), *Observation of Exclusive Gamma Gamma Production in $p\bar{p}$ Collisions at $\sqrt{s} = 1.96\text{ TeV}$* , Phys. Rev. Lett. **108** (2012) 081801, arXiv:1112.0858 [hep-ex].
 - [20] G. Baur, K. Hencken, D. Trautmann, S. Sadovsky, and Y. Kharlov, *Coherent $\gamma\gamma$ and $\gamma - A$*

- interactions in very peripheral collisions at relativistic ion colliders*,
Phys. Rept. **364** (2002) 359–450, arXiv:hep-ph/0112211 [hep-ph].
- [21] C. A. Bertulani, S. R. Klein, and J. Nystrand, *Physics of ultra-peripheral nuclear collisions*,
Ann. Rev. Nucl. Part. Sci. **55** (2005) 271–310, arXiv:nucl-ex/0502005 [nucl-ex].
 - [22] A. J. Baltz, *The Physics of Ultraperipheral Collisions at the LHC*, Phys. Rept. **458** (2008) 1–171,
arXiv:0706.3356 [nucl-ex].
 - [23] D. Bardin, L. Kalinovskaya, and E. Uglov, *Standard Model light-by-light scattering in SANC:
analytic and numeric evaluation*, Phys. Atom. Nucl. **73** (2010) 1878–1888,
arXiv:0911.5634 [hep-ph].
 - [24] T. Hahn and M. Perez-Victoria, *Automatized one loop calculations in four-dimensions and
D-dimensions*, Comput. Phys. Commun. **118** (1999) 153–165, arXiv:hep-ph/9807565 [hep-ph].
 - [25] G. J. van Oldenborgh and J. A. M. Vermaseren, *New Algorithms for One Loop Integrals*,
Z. Phys. **C46** (1990) 425–438.
 - [26] G. Passarino and M. Veltman, *One Loop Corrections for e^+e^- Annihilation Into $\mu^+\mu^-$ in the
Weinberg Model*, Nucl. Phys. **B160** (1979) 151.
 - [27] B. L. Ioffe, V. A. Khoze, and L. N. Lipatov, *Hard Processes. Vol. 1: Phenomenology, Quark
Parton Model*. 1985. Amsterdam, Netherlands: North-holland (1985) .
 - [28] M. Khusek, W. Schäfer, and A. Szczurek, *Exclusive production of $\rho^0\rho^0$ pairs in gamma gamma
collisions at RHIC*, Phys. Lett. **B674** (2009) 92–97, arXiv:0902.1689 [hep-ph].
 - [29] A. Donnachie and P. V. Landshoff, *Total cross-sections*, Phys. Lett. **B296** (1992) 227–232,
arXiv:hep-ph/9209205 [hep-ph].
 - [30] A. Donnachie, H. G. Dosch, P. V. Landshoff, and O. Nachtmann, *Pomeron physics and QCD*,
Camb. Monogr. Part. Phys. Nucl. Phys. Cosmol. **19** (2002) 1–347.
 - [31] A. Szczurek, N. N. Nikolaev, and J. Speth, *From soft to hard regime in elastic pion pion
scattering above resonances*, Phys. Rev. **C66** (2002) 055206, arXiv:hep-ph/0112331 [hep-ph].
 - [32] M. Khusek-Gawenda and A. Szczurek, *Exclusive muon-pair productions in ultrarelativistic
heavy-ion collisions – realistic nucleus charge form factor and differential distributions*,
Phys. Rev. **C82** (2010) 014904, arXiv:1004.5521 [nucl-th].
 - [33] M. Khusek-Gawenda, A. Szczurek, M. V. T. Machado, and V. G. Serbo, *Double – photon
exclusive processes with heavy quark – heavy antiquark pairs in high-energy Pb-Pb collisions at
LHC*, Phys. Rev. **C83** (2011) 024903, arXiv:1011.1191 [nucl-th].
 - [34] M. Khusek-Gawenda and A. Szczurek, *Exclusive production of large invariant mass pion pairs in
ultraperipheral ultrarelativistic heavy ion collisions*, Phys. Lett. **B700** (2011) 322–330,
arXiv:1104.0571 [nucl-th].
 - [35] S. Baranov, A. Cisek, M. Khusek-Gawenda, W. Schäfer, and A. Szczurek, *The $\gamma\gamma \rightarrow J/\psi J/\psi$ reaction and the $J/\psi J/\psi$ pair production in exclusive ultraperipheral ultrarelativistic heavy ion
collisions*, Eur. Phys. J. **C73** no. 2, (2013) 2335, arXiv:1208.5917 [hep-ph].
 - [36] M. Khusek-Gawenda and A. Szczurek, *$\pi^+\pi^-$ and $\pi^0\pi^0$ pair production in photon-photon and
in ultraperipheral ultrarelativistic heavy ion collisions*, Phys. Rev. **C87** no. 5, (2013) 054908,
arXiv:1302.4204 [nucl-th].
 - [37] M. Khusek-Gawenda and A. Szczurek, *Double-scattering mechanism in the exclusive
 $AA \rightarrow AA\rho^0\rho^0$ reaction in ultrarelativistic collisions*, Phys. Rev. **C89** no. 2, (2014) 024912,
arXiv:1309.2463 [nucl-th].
 - [38] (ATLAS Collaboration), *Zero degree calorimeters for ATLAS*,.
 - [39] O. A. Grachov *et al.*, (CMS Collaboration), *Performance of the combined zero degree calorimeter
for CMS*, J. Phys. Conf. Ser. **160** (2009) 012059, arXiv:0807.0785 [nucl-ex].